

Study on the static properties and energy evolution mechanism of rock-concrete composites

Shang Hui, Xu Ying, Yu Lei'lei

School of Civil Engineering and Architecture, Anhui University of Science & Technology, China

ABSTRACT: *In order to study the static mechanical relationship between rock-concrete assemblies and their components, the stress-strain characteristics, peak stress, strain and compression damage energy evolution laws of rock, concrete and rock-concrete assemblies were analysed by indoor uniaxial compression tests. The results show that the stress-strain curves of different rock-concrete composites are similar in uniaxial compression, their peak strengths and moduli of elasticity reside between the two components, which are greatly affected by the uniaxial compressive strength and modulus of elasticity of concrete, and their peak strains are enhanced significantly compared with those between the components, which are greatly affected by the peak strains of rock; Under the same strain conditions, the laws of total energy and energy absorption rate of rock, concrete and rock-concrete assemblies are consistent with those of their uniaxial compressive strengths, and the total energy absorbed by concrete specimens has a greater influence on the total energy absorbed by assemblage specimens. The results of the study can provide a reference for the study of the static mechanical properties of rock-concrete composite structures.*

Keywords: *rock-concrete composites, mechanical properties, energy evolution*

Date of Submission: 27-08-2024

Date of Acceptance: 05-09-2024

I. INTRODUCTION

The interaction between concrete gravity dam and dam foundation, arch dam and dam shoulder in large-scale water conservancy projects, the supporting structure and surrounding rock in underground projects such as deep resource extraction and tunnel construction, and the interaction between ultra-high-rise buildings, underground space structures and foundations in civil engineering projects can be categorised as the interaction between two components of typical rock-concrete assemblages, which is an important issue concerning the stability of various types of engineering bodies[13]. Therefore, it is of great significance to study the interaction mechanism between the two components of rock-concrete composite.

In the intersection of civil engineering and materials science, the study of static mechanical properties of binary materials has been the focus of scientists. With the continuous development of research techniques and theories, foreign scholars have explored the mechanical behaviours in these materials through various experimental methods and made a series of important discoveries. Lu, Jianyou et al.[46]In order to study the effects of different combination modes, interface angles, interface roughness, and prefabricated cracks on the mechanical and destructive characteristics of the assemblage, static load/cycle radial compression tests were conducted on the rock-concrete assemblage to obtain the fracture modes of the assemblage under different interface inclinations, and the relationship between the peak load and the combination mode, the cycle times, and the interfacial groove depths (widths).Kishen et al.[7]obtained the interfacial fracture energy of limestone-concrete composites more severe than the strength discount by wedge splitting test. Zuo Jianping et al.[8]conducted uniaxial and triaxial tests on combined body specimens of coal and rock at 0° combined interface to obtain their overall compressive strength and damage mechanism. Liu J et al.[9] studied the damage process, damage characteristics and stress-strain characteristics of different coal and rock masses under uniaxial compression, and analyzed the influence of mechanical strength on the mechanical behavior of combined samples. W. Dong et al.[10] respectively conducted uniaxial tensile test and three-point bending test on rock-concrete composite materials, obtained the damage evolution law at the interface of rock-concrete composite materials, and verified it by numerical simulation method. Yang Lei et al. [11] conducted uniaxial compression tests on coal, rock and coal-rock combination under cyclic loading and unloading, compared the energy evolution law of coal-rock combination samples, and determined the damage mechanism of the combination.

In summary, the static mechanical properties of rock-concrete compositions have been studied at home and abroad, but the mechanical properties of rock-concrete compositions and the law of energy evolution of compressive damage are still unclear. Therefore, this paper takes Ordos sandstone, concrete and rock-concrete assemblage in Inner Mongolia as the research objects, and carries out uniaxial compression tests of rock, cement

mortar concrete, high-performance concrete, rock-cement mortar concrete and rock-high-performance concrete to analyse the stress-strain characteristics, peak stress, strain and elastic modulus laws. At the same time, the energy absorption, storage and dissipation modes of each specimen were characterized by the energy evolution principle of compressive fracture process. The results of the study can provide references for the static properties of rock-concrete composites.

II. SPECIMEN PREPARATION AND EXPERIMENTAL EQUIPMENT

2.1 Specimen Preparation

The materials used in this study include rock, cement, silica fume, water reducer, river sand, water and fly ash. The rock samples are taken from Ordos sandstone in Inner Mongolia, and the cement is conch P-O42.5 Portland cement. According to the multiple proportioning experiments conducted by orthogonality experiments, the proportioning of ordinary concrete and high-performance concrete specimens was selected as shown in Table 1. The rock-concrete assemblage specimens used in the experiments were all formed by pouring cement mortar and rock specimen specimens under natural conditions in the ratio of 1:1, as shown in Fig. 1. The specific production method is as follows: the sandstone specimen is polished smooth with fine sandpaper to minimize the effect of the error generated by the interface roughness, and put it into a 50*100mm mould, and then the cement mortar configured according to the ratio in Table 1 is stirred in a high-speed mixer for about 10 min, and when the cement mortar is completely reacted, it is poured into a mould with rocks, and then vibrated on a vibrating table at an appropriate frequency for about 2 min, until the mortar is completely reacted. After the mortar was fully reacted, it was poured into the mould with rocks and vibrated on a vibrating table at a suitable frequency for about 2 min, and the vibration was stopped when the air bubbles in the mortar were completely overflowed. After 24 h of resting, the moulds were removed and the specimens were transferred to a special high-temperature curing box for 14 days, after which they were taken out and polished, and the specimens were finished.

Table 1 Concrete ratios

| groups | Cement/g | Silica fume/g | Coal ash/g | River sand/g | Water/ml | water reducing agent/g |
|---------------------------|----------|---------------|------------|--------------|----------|------------------------|
| High-performance concrete | 924 | 176 | 150 | 997 | 190 | 20 |
| Cement mortar concrete | 1100 | -- | -- | 1100 | 400 | -- |

Where R is a complete rock specimen, S1 is a complete high-performance concrete specimen of the first proportion; S2 is a complete cement mortar concrete specimen of the second proportion; Z1 is a rock-high-performance concrete composite specimen; and Z2 is a rock-cement mortar concrete specimen.

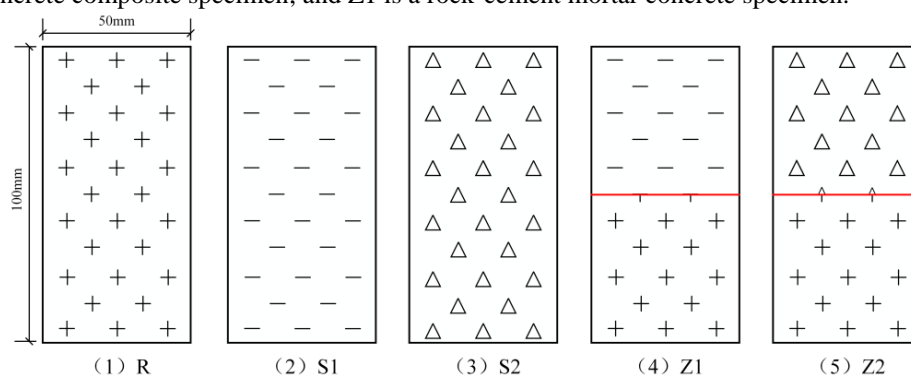


Figure 1 Schematic diagram of test piece

2.2 Experimental Equipment

The experimental equipment adopts WAW-1000 microcomputer controlled electro-hydraulic servo universal testing machine of State Key Laboratory of Anhui University of Science and Technology. The experimental equipment is shown in Figure 2. The experimental control mode is displacement control, the force range is 100 kN, the displacement end point is 3.00 mm, the force limit is 80 kN, the displacement range is 5.00 mm, the displacement rate is 0.2 mm/min, and the displacement limit is 3.1 mm.



Figure 2 WAW-1000 microcomputer controlled electro-hydraulic servo universal testing machine

III. UNIAXIAL COMPRESSION TEST RESULTS AND ANALYSES

The relationship between uniaxial compressive strength, axial peak strain and deformation parameters of rock, concrete and rock-concrete composite specimens is shown in Table 2.

Table 2 Mechanical parameters of specimens under uniaxial compression

| groups | Uniaxial compressive strength σ_r / MPa | Peak axial strain $\epsilon_r/10^{-3}$ | Modulus of elasticity E/GPa | Modulus of deformation E_{50} /GPa |
|--------|---|---|--------------------------------|---|
| R | 64.87 | 12.32 | 7.18 | 4.27 |
| S1 | 46.25 | 11.24 | 5.74 | 2.88 |
| S2 | 25.62 | 9.65 | 3.96 | 2.12 |
| Z1 | 58.65 | 14.33 | 6.75 | 3.64 |
| Z2 | 40.12 | 12.20 | 4.32 | 2.67 |

It can be seen from Table 2 that under uniaxial compression, the mechanical parameters of rock R, concrete S1, S2 and assemblage Z1 and Z2 are also different due to the different material ratio of specimens. Among them, the uniaxial compressive strength, elastic modulus and deformation modulus of specimen R are the largest, followed by Z1, S1, Z2 and S2. The axial peak strain modes of specimens are slightly different, and the size sequence of specimens Z1, R, Z2, S1 and S2 is Z1, R, Z2, S1 and S2. The uniaxial compressive strength of specimen Z1 is in the middle of specimen R and specimen S1, reaching 90% of the compressive strength of specimen R and 126.8% of the compressive strength of specimen S1. The uniaxial compressive strength of specimen Z2 is between that of specimen R and S2, reaching 61.8% of the compressive strength of specimen R and 156.6% of the compressive strength of specimen S2. It can be seen that the compressive strength, peak strain, elastic modulus and deformation modulus of rock-concrete composite decrease with the decrease of compressive strength of concrete material. When the compressive strength difference between rock and concrete material is large, the compressive strength of the combination of the two will be closer to the compressive strength of the concrete material with low strength. Therefore, improving the strength of concrete is one of the most powerful ways to improve the strength of composite specimens.

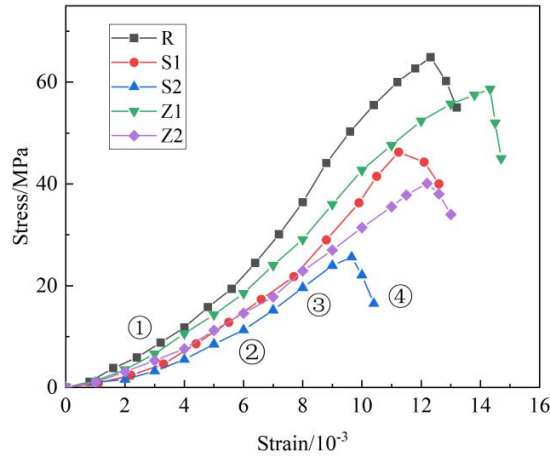


Fig. 3 Stress-strain curve of specimens under uniaxial compression

It can be seen from the stress-strain curve of specimens in FIG. 2 that rock, concrete and assemblages all show brittle fracture under uniaxial compression, and when the axial stress on specimens reaches its peak, the stress-strain curve drops sharply, indicating that all specimens are brittle materials. According to the stress-strain curve, the damage process of the specimen can be divided into four stages: initial internal pore closing stage, elastic deformation stage, crack propagation stage and strain softening stage. When the specimen is in the first stage ①: inner hole closure stage, the original inner hole is gradually closed due to the continuous axial load, resulting in a nonlinear stress-strain curve, in which the initial inner hole closure stress of rock, concrete and specimen combination is about $0.3\sigma_r$, $0.2\sigma_r$ and $0.24\sigma_r$, respectively. With the continuous increase of axial load, the original internal pores are closed, and the sample is completely closed, but if the original pores are not closed, the sample is not closed. With the continuous increase of axial load, the original pores inside the specimen were completely closed, and the specimen entered the second stage ②: elastic deformation stage, and the stress-strain curve showed a linear relationship. As the axial load continued to increase, the specimen began to appear slight cracks, and the specimen entered the third stage ③: crack propagation stage. At this time, stress concentration appeared around the crack, the crack gradually expanded, and the stress-strain curve of the specimen gradually deviated from the elastic deformation trend. The cracking stress of rock, concrete and specimen combination was about $0.6\sigma_r$, $0.5\sigma_r$ and $0.5\sigma_r$, respectively. When the specimen reaches the fourth stage ④: strain softening stage, the macroscopic cracks appear rapidly, and the stress-strain curve decreases rapidly after the peak value. At this time, the specimen can only withstand low axial stress.

IV. ENERGY EVOLUTION LAW IN THE DESTRUCTION PROCESS OF COMPRESSION DEFORMATION

The deformation and failure of binary body under external load is a dynamic evolution process of energy input, accumulation and dissipation. The initiation and propagation of cracks are accompanied by energy dissipation. Therefore, the analysis of deformation and damage processes of rock, concrete and rock-concrete composite rock samples based on energy perspective is the key to reveal the relationship between their mechanical properties.

4.1 Principle of Energy Calculation

According to the first law of thermodynamics, the input energy (work done by external forces) of the specimen under uniaxial compression is mainly converted into elastic energy and dissipative energy, and the input energy, elastic energy and dissipative energy of the specimen can be calculated according to the formula. [12](1~3).

$$U = \int \sigma d\varepsilon \quad (1)$$

$$U_e = \sigma^2 / (2E) \quad (2)$$

$$U_d = U - U_e = \int \sigma d\varepsilon - \sigma^2 / 2E \quad (3)$$

where: U , U_e and U_d are the input, elastic and dissipation energies, respectively, MJ/m^3 ; and E is the tangential elastic modulus, GPa .

4.2 Energy Evolution Law

Based on the equation. (1~3), the total energy, elastic strain energy, dissipated energy of rock, concrete and rock-concrete combination and the variation law of each energy at the peak point can be calculated, as shown in Figure 4.

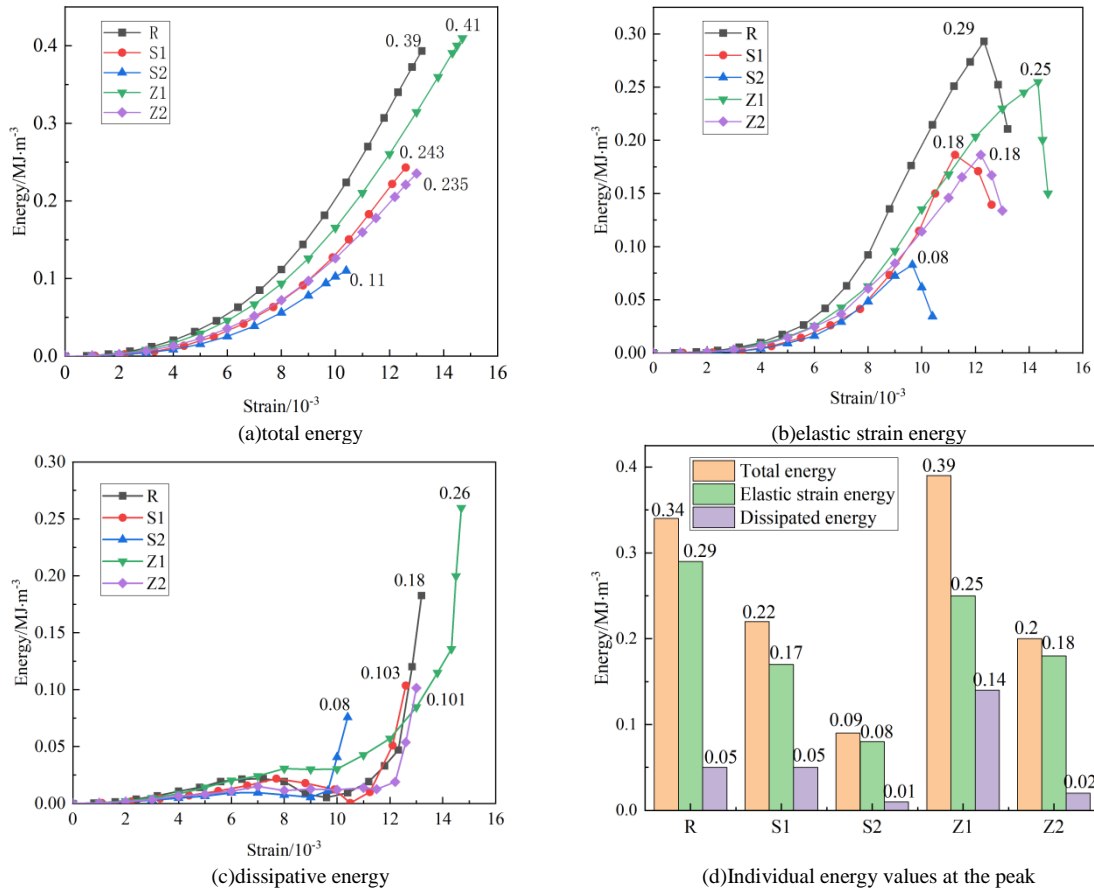


FIGURE 4: Evolution law of each energy of specimens

As can be seen from FIG. 4, due to the different material ratios of specimens, the energy absorption, storage and release of rock R, concrete S1, S2, and assemblages Z1 and Z2 during loading and damage are significantly compared. It can be seen from FIG. 4(a) that under the same strain condition, the total energy and energy absorption rate of sample R are greater than those of other samples, followed by Z1, S1, Z2 and S2. The variation law of total energy and energy absorptivity of specimens under the same strain condition is consistent with that of uniaxial compressive strength. The strain of specimen Z1 is greater than that of specimen R, and the total energy absorbed by specimen Z1 is also greater than that of specimen R. The total energy absorbed by specimen Z2 is between specimen R and specimen S2, which is more than twice the energy absorbed by specimen S2, indicating that the combined structure of rock and concrete can absorb more energy than a single concrete structure. The total energy absorbed by specimen Z1 is much larger than that of specimen Z2, indicating that the total energy absorbed by concrete has a greater influence on the total energy absorbed by composite materials. Therefore, increasing the strength of concrete can improve the total energy and energy absorption rate of composite specimens.

It can be seen from Figure 4(b) that the elastic strain energy curves of rock, concrete and composite specimens are highly correlated with their stress-strain curves. With the increase of strain, the elastic strain energy of each sample increases slowly at first and then rapidly. When the stress loading reaches the peak compressive strength of the sample, the elastic strain energy reaches the peak value and the elastic strain energy curve decreases rapidly. Under the same strain condition, the peak value of elastic strain energy of sample R is higher than that of other samples, followed by Z1, S1, Z2 and S2. The elastic strain energy storage of specimens Z1 and Z2 is between specimens R, S1 and R, S2, and the elastic strain energy storage of specimen Z2 is more than twice that of specimen S2, indicating that the combined rock and concrete structure can store more energy than a single concrete structure. The storage elastic strain energy of specimen Z1 is much higher than that of

specimen Z2, indicating that the storage elastic strain energy of concrete has a great influence on the elastic strain energy of composite materials.

It can be seen from FIG. 4(c) that the energy dissipation of rock, concrete and composite specimens remains basically unchanged at the beginning of stress loading. When the stress load reaches the peak compressive strength of the specimen, the dissipative energy curve of the specimen increases rapidly and reaches the peak dissipative energy. The peak dissipative energy of specimen Z1 is greater than that of other specimens, followed by R, S1, Z2 and S2, indicating that the small strength difference between rock and concrete increases the peak dissipative energy of the combined structure and enhances the energy dissipation phenomenon during the damage process. When the strength difference between rock and concrete is large, the peak dissipative energy of rock-concrete composite specimen is small.

As can be seen from FIG. 4 (d), the total energy, ultimate energy storage and ultimate dissipative energy of rock, concrete and composite specimens at peak points are as follows: Total energy :Z1>R>S1>Z2>S2; Limit energy storage :R>Z1>S1>Z2>S2; Limiting dissipation energy Z1>R>S1>Z2>S2. The results show that when the strength difference between rock and concrete is small, the total energy and final dissipated energy at the peak of rock-concrete composite increase. When the strength difference between rock and concrete is large, the total energy, ultimate energy storage and ultimate dissipative energy at the peak of rock-concrete specimen increase little. Therefore, increasing the concrete strength can increase the total energy, ultimate energy storage and ultimate dissipative energy at the peak of the composite sample.

V. RESULTS

The stress-strain characteristics, peak stress, strain and compressive damage energy evolution of rock, concrete and rock-concrete composite materials were analyzed through laboratory uniaxial compression tests. The results are as follows:

(1) The compressive strength, peak strain, elastic modulus and deformation modulus of rock-concrete composite decrease with the decrease of compressive strength of concrete material; When the difference between the compressive strength of rock and concrete is large, the compressive strength of the combination of rock and concrete is closer to the compressive strength of the concrete material with low strength.

(2) The damage process of the specimen is divided into the initial internal pore closure stage, elastic deformation stage, crack extension stage and strain softening stage. Among them, the initial internal pore closure stresses of rock, concrete and assemblage specimens are about $0.3\sigma_r$, $0.2\sigma_r$ and $0.24\sigma_r$, respectively, and the crack initiation stresses are about $0.6\sigma_r$, $0.5\sigma_r$ and $0.5\sigma_r$, respectively.

(3) Under the same strain conditions, the laws of total energy and energy absorption rate of rock, concrete and rock-concrete assemblies are consistent with their uniaxial compressive strength and modulus of elasticity laws, and the combined structure of rock and concrete can absorb more energy than a single concrete structure, and the total energy absorbed by concrete specimens has a greater effect on the total energy absorbed by assemblies specimens.

(4) When the difference between rock and concrete strengths is small, it will increase the total energy and ultimate dissipated energy at the peak point of rock-concrete combination; when the difference between the two is large, the enhancement of the total energy, ultimate energy storage and ultimate dissipated energy at the peak point of rock-concrete specimen is small.

REFERENCES

- [1] XIE H P, CHEN Z H, ZHOU H W, et al. Study on two-body mechanical model based on interaction between structural body and geo-body[J]. Chinese Journal of Rock Mechanics and Engineering, 2005(09):1457-1464.
- [2] VIZINI V O S, FUTAI M M. Mode II fracture toughness determination of rock and concrete via Modified Direct Shear Test[J]. Engineering Fracture Mechanics, 2021, 257:108007.
- [3] TIAN J, WU X, WANG W W, et al. Experimental study and mechanics model of ECC-to-concrete bond interface under tensile loading[J]. Composite Structures, 2022, 285:115203.
- [4] LU J Y. Study on mechanical properties of rock-concrete disc under radial compression[D]. Henan: Henan Polytechnic University, 2018.
- [5] ZHOU Z L, LU J Y, CAI X. Static and dynamic tensile behavior of rock-concrete bi-material disc with different interface inclinations[J]. Construction and Building Materials, 2020, 256: 119424.
- [6] CHANG X, GUO T F, LU J Y, et al. Experimental study on rock-concrete joints under cyclically diametrical compression[J]. Geomechanics and Engineering, Daejeon: Techno-Press, 2019, 17(6): 553-564.
- [7] Kishen J M C, Saouma V E. Fracture of rock-concrete interfaces: laboratory tests and applications[J]. Structural Journal, 2004, 101(3): 325-331.
- [8] ZUO J P, XIE H P, WU A M. Investigation on failure mechanisms and mechanical behaviors of deep coal-rock single and body and combined body[J]. Journal of Rock Mechanics and Engineering, 2011, 30(01): 84-92.
- [9] LIU J, Wang E Y, SONG D Z, et al. Effects of rock strength on mechanical behavior and acoustic emission characteristics of samples composed of coal and rock [J]. Journal of China Coal Society, 2014, 39(4): 685-691.

- [10] Dong W, Wu Z, Zhou X. Fracture mechanisms of rock-concrete interface: experimental and numerical[J]. Journal of Engineering Mechanics, 2016, 142(7): 04016040.
- [11] YANG Lei, GAO Fu-qiang, WANG Xiao-qing, et al. Energy evolution law and failure mechanism of coal-rock combined specimen[J]. Journal of China Coal Society, 2019, 44(12): 3894-3902.
- [12] FU Qiang,ZHAO Xu,HE Jiaqi,et al.Constitutive Response of Hybrid Basalt-polypropylene Fiber-reinforced Concrete Based on Energy Conversion Principle[J].Journal of Chinese Ceramic Society,2021,49(08):1670-1682.